Platinum dispersion analysis depending on the pore geometry of the support

Wilfried Gille[a,*], Dirk Enke[b], Frank Janowski[b], and Thomas Hahn[b]

[a] *Martin-Luther-University Halle-Wittenberg, Department of Physics, SAS Laboratory, Hoher Weg 8, D-06120 Halle, Germany*
[b] *Martin-Luther-University Halle-Wittenberg, Department of Technical Chemistry, Institute of Technical and Macromolecular Chemistry, Schloßberg 2, D-06108 Halle, Germany*

Received 15 July 2003; accepted 5 August 2003

Two 0.1wt% Pt-porous glass catalysts have been characterized: mesopores formed by finely dispersed colloidal silica inside a macroporous glass, and micropores defined by the porous glass itself. Introducing the so-called range order length parameter L, chord length analysis for $L = 5$ nm yields specific structure parameters of the metal particles inside both catalyst supports (dispersion, specific metal surface areas, basic arrangement, size distribution and volume fraction). The pore size available basically differs with both pore systems. In the one case an unlimited three-dimensional growth, and, in the other one a limited two-dimensional growth of small Pt-crystallites have been detected. The corresponding particle size distributions $f(d)$ and $f(H)$ have been determined.

KEY WORDS: Pt-catalyst; dispersion; range order; chord length analysis.

1. Introduction

There is great interest in preparing metal nanoparticles with controlled size and shape supported on or encapsulated in porous silica [1,2]. Particle sizes and particle size distributions of metal-supported catalysts influence the activity in structure sensitive reactions and their selectivity in multipath reactions. The reliable determination of particle sizes, size distributions, metal specific surface areas and dispersions is of particular importance. There is a number of different methods that can be applied to estimate these parameters, e.g. volumetric gas adsorption and electron microscopy. Small-angle X-ray scattering (SAS) is another suitable method. Different experimental techniques, e.g. anomalous SAS [3] or support pore packing by a liquid whose electron density is close to that of the support material have been in use [4,5].

It is one aim in industrial application to reduce the Pt-content without reduction of the activity of the resulting supported catalyst. Specific surface areas of Pt-particles of 100 $m^2\ g^{-1}$ are typical [6]. In our investigations, the inserted platinum content was 0.1 wt% [7]. The so-called SAS correlation function (CF) $\gamma(r) \equiv \gamma(r, L)$ is defined in terms of the isotropic SAS intensity $I(h)$ via numerical procedures [8–10]. The CF can be interpreted in terms of the electron density fluctuation on a selected length scale, $r < L$. This should yield specific results for size and geometry of the Pt-particles.

The isotropic scattering intensity $I(h)$ $(h = 4\pi/\lambda \cdot \sin(\theta)$, scattering vector h, wavelength λ and scattering angle 2θ) is a superimposition: The single metal nanometer-particles, their packing and the porous system contribute to $I(h)$, given in terms of $\gamma(r, L)$,

$$I(h) = \frac{\int_0^L r^2 \gamma(r, L) \cdot \sin(h \cdot r)/(h \cdot r) \mathrm{d}r}{\int_0^L r^2 \gamma(r, L) \mathrm{d}r}. \qquad (1)$$

A suitable, sufficiently small parameter L allows to detect and study the metal particles via chord length analysis [11–13]. By this way the influence of the scattering of the support can be limited.

The volume fraction $c = c(L)$ of an isotropic two-phase system depends on the range order L [14,15]. Let $S/V = S(L)/V$ be the specific surface area. The lengths, $\bar{l}$ and $\bar{m}$ are the first moments of the chord length distribution density (CLD) of the (non-connected) particle phase $\phi(l)$ and of the connected intermediate space (connected phase) $f(m)$, respectively. A sequence of stereological parameters are closely interrelated,

$$c(L) = \frac{\bar{l}(L)}{\bar{l}(L) + \bar{m}(L)},$$
$$|\gamma'(0, L)| = \frac{1}{l_p(L)} = \frac{1}{\bar{l}(L)} + \frac{1}{\bar{m}(L)} = \frac{S(L)}{V \cdot c(L) \cdot [1 - c(L)]}. \qquad (2)$$

Rosiwal, see [15], published $c = \bar{l}/(\bar{l} + \bar{m})$ in 1898. equations (1) and (2) connect $c(L)$ and the SAS experiment for a selected L-region. Linear simulation models approximate the geometry of the sample, where $\gamma''(r, L)/|\gamma'(0, L)| = \gamma''(r, L) \cdot \bar{l} \cdot (1 - c) = \gamma''(r, L) \cdot \bar{m} \cdot c$ involves the sequences of multi chord distributions and one chord distributions [11].

* To whom correspondence should be addressed.
E-mail: gille@physik.uni-halle.de

1011-372X/04/0300–0013/0 © 2004 Plenum Publishing Corporation

In our experiments, the Pt-crystal structure ($L \rightarrow 0.5$ nm, fcc lattice, $a = 0.392$ nm) has not been investigated. The Pt-density, $\rho \approx 21$ g cm^{-3}, allows to connect S_V with the Pt-mass [16]. The surface area of a single Pt-atom is $S_0 \approx 8.9 \cdot 10^{-20}$ m^2.

2. Experimental

Two different porous glasses were prepared, a sodium borosilicate initial glass (composition 70 wt% SiO_2, 23 wt% B_2O_3, 7 wt% Na_2O) in shape of beads (0.1–0.2 mm in diameter) were phase-separated at 630 °C for 24 h (G1) and at 530 °C for 7 h (G2), respectively.

After leaching the initial glass G1 with 3 N hydrochloric acid at 90 °C for 40 h the first support (S1) resulted. The second support (S2) was obtained by leaching the initial glass G2 with 3 N hydrochloric acid at 90 °C for 15 h.

The supports S1 and S2 were impregnated in vacuum by use of H_2PtCl_6 – solution, resulting in a metal load of 0.1 wt% Pt. Then, the impregnated catalysts were dried in air at 80 °C for 24 h. Finally, the samples were reduced in H_2 stream (3.5 L h^{-1}) at 300 °C for 3 h (heating rate 2 K min^{-1}). So, S1(Pt) and S2(Pt) resulted. The abbreviations, S1, S1(Pt), and S2, S2(Pt), will be used.

A Kratky camera (nickel-filtered CuK_α-radiation), was used for recording $I(h)$, from 0.008 nm^{-1} up to $h_{max} = 3.8$ nm^{-1}. The functions $\gamma(r,L)$, $\gamma'(r,L)$, and $\gamma''(r,L)$ were obtained (inversion of equation (1)) and analyzed. For determining the Pt-particle size distribution of S1(Pt), $L_0 = 10$ nm was inserted into equation (1). In the other cases, $L = 5$ nm was operated with.

By use of a Sorptomatic 1900 Turbo apparatus by Carlo Erba Instruments, nitrogen sorption measurements were performed. The samples were degassed at 393 K before measurement for at least 24 h at (10–5) mbar.

Adsorption and desorption isotherms were recorded over relative pressures $0 < P/P_0 < 1$. Surface areas were determined by the BET method, assuming that the area of a nitrogen molecule is 0.162 nm^2 [17]. The total pore volumes result from the amount of gas adsorbed at a relative pressure $P/P_0 = 0.99$ assuming that the pores are filled with condensed adsorptive in the normal liquid state.

3. Results

Sample S1 shows a typical type IV isotherm shape with hysteresis of type H2 (IUPAC classification), characteristic of mesoporous materials (figure 1). The mesopores result from colloidal silica in the macropores of the main silica framework of the porous glass [7,11]. Texture characteristics of the porous glass supports are included in table 1.

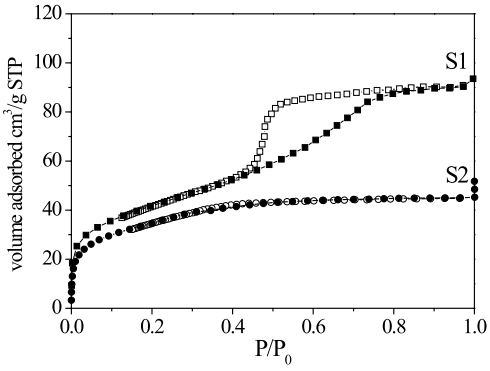

Figure 1. N_2 sorption isotherms of porous glasses used as supports S1 and S2.

The shape of the isotherm of sample S2 (figure 1) indicates that the pore system is mainly formed by wider micropores or supermicropores (pores of width >1 nm) [18].

Considering relatively small h, the differences in the scattering behaviour between S1/S1(Pt) and S2/S2(Pt) are not significant. This is not surprising. On the length scale of the basic porous structure, the Pt-particles are unessential. However, $I(h)$ of the support samples is higher than that of the pure carrier materials. This can be traced back to the Pt-content [6–8]. The function $\gamma(r) = \gamma(r,L)$ has been analyzed for $\pi/h_{max} < r < L$.

The CF of S1(Pt) possesses a local minimum of $\gamma(r_{min})$, typical of tightly packed hard particles (Pt-crystallites), at $r_{min} \approx 2.2$ nm. The function γ'' possesses a minimum at $r \approx 3.8$ nm and $\bar{l} \approx 1.4$ nm, $\bar{m} \approx 2.4$ nm result from γ''. Thus, the information about the Pt-particles is fully included in the interval $r < 3.8$ nm. The sum $\bar{l} + \bar{m} \approx 3.8$ nm reflects the minimum of γ''.

Table 1
Basic textural parameters

Support	Mesoporous glass S1	Microporous glass S2
Long order range analysis:	20 nm < L < 100 nm	20 nm < L < 100 nm
Specific surface area	$A_S \approx 150$ m^2 g^{-1}	$A_S \approx 124$ m^2 g^{-1}
Specific pore volume	$V_p \approx 145$ cm^3 g^{-1}	$V_p \approx 0.07$ cm^3 g^{-1}
Average pore diameter	$\bar{d}_p = 6$ nm	$\bar{d}_p = 2.3$ nm
Porosity, (L = 20 nm)	C = 0.24	C = 0.13
Short order range analysis:	L = 5 nm, L_0 = 10 nm	L = 5 nm
Pt-crystallites	$c(L) \approx 0.4$	$c(L) \approx 0$
Size of Pt-crystallites	Random diameter d	Random height H
Mean size	$\bar{d} = 2.8$ nm	$\bar{H} = 0.8$ nm
Type of distribution	Equation (3)	Equation(4)
Pt-dispersion	D = 0.15	D = 0.4
Specific Pt-surface area	$\frac{s}{m} = (40 \pm 10) m^2\ g^{-1}$	$\frac{s}{m} \approx 100 m^2\ cg^{-1}$
The ratio S/V	$\frac{s}{V} \approx 1$ nm^{-1}	$\frac{s}{V} \approx 2.5$ nm^{-1}
Porod's parameter l_P	l_P = 1.1 nm	l_P = 1.5 nm
Mean chord lengths	$\bar{l} = 1.4$ nm; $\bar{m} = 2.4$ nm	$\bar{l} \approx 2\,\bar{H} = 1.5$ nm; $\bar{m} \gg \bar{l}$

The mean volume fraction of the Pt-particles inside a typical L^3 test cube is $c = \bar{l}/(\bar{l} + \bar{m}) = 1.4/3.8 \approx 40\%$. This refers to a relatively close packing of single groups of Pt-particles. From this volume density of Pt (at selected places), the specific surface area of the metal results, see equation (2). It follows $S/V \approx 1/\text{nm}^{-1}$, which yields $S/m = (40 \pm 10)\ \text{m}^2\ \text{g}^{-1}$. Finally, the dispersion D of the Pt-atoms $S_0/m = 275\ \text{m}^2\ \text{g}^{-1}$ follows. Thus $D = 40/275 \approx 0.15$. For a check, the behaviour of $\gamma(r, L)$ can be approximated by a so-called linear simulation model (parameters $\bar{l} = 1.4$ nm, $\bar{m} = 2.4$ nm, $L = 5$ nm) [7,14].

The nearly spherical Pt-particles vary in size. Let d be their random diameter. The size distribution density $f(d)$, see the theory in [19,20], of the random Pt-particle diameters d results (see figure 2). Inserting the selected, larger length scale parameter $L = L_0 = 10$ nm, the mathematical precondition of non-interacting spheres is nearly fulfilled. Here, $f(d) \equiv 0$, if $L_0 < d$ and no basic mathematical type of $f(d)$ has been inserted *a priori*. A highly unsymmetrical $f(d)$ results (figure 2). However, $f(d)$ fits with several so-called standard distribution densities.

The dashed line results, approximating $f(d)$ by a *log normal distribution density*

$$f(d) = \frac{1}{\sqrt{2\pi}\sigma d} \cdot \exp\left(-\frac{(\ln(d) - \mu)^2}{2\sigma^2}\right), \qquad (3)$$

with parameters $\sigma = 0.27\ \text{nm}^{-1}$ and $\mu = 0.98$. The first moments are $\text{M1} = \bar{d} = 2.76$ nm and $\text{M2} = 8.2\ \text{nm}^2$.

In fact, equation (3) is connected with the mean chord length inside a Pt-crystallite: Applying the rule $\bar{l} = 2d/3$ (mean chord length of a single sphere of diameter d), the estimation $\bar{d} \approx 2.1$ nm follows.

For S2(Pt) $\gamma'(0) = -1/(1.5\ \text{nm})$ [7]. Compared with the last section, the differences between S2/S2(Pt) are smaller. The CF of S2 is nearly a straight line, however $\gamma(r)$ of S2(Pt) possesses a maximum curvature at

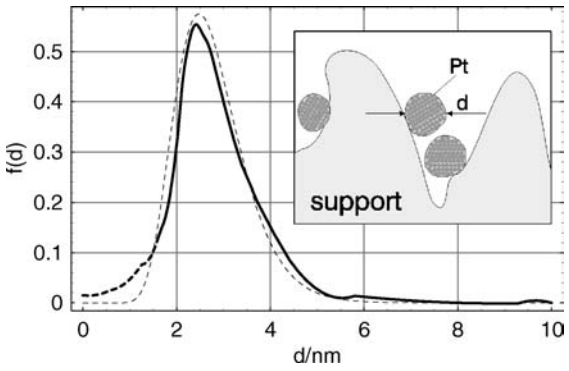

Figure 2. Size distribution density $f(d)$ of the random diameter of Pt-particles (thick line). A fit of the density obtained operating with equation (3) (thin, continuously dashed line).

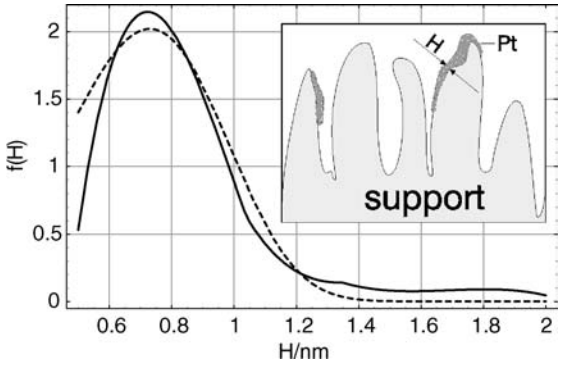

Figure 3. Size distribution density $f(H)$ of the random Pt-skin height (thick line). An approximation with a selected distribution density yields $\mu = 0.73$ nm (thin, continuously dashed line).

$r = r_s \approx 0.8$ nm. From the analysis of the structure function $r \cdot \gamma(r)$, see [7,8,21], the estimation of very thin platelike metal particles is compelling. Here, $\gamma_p(r, H)$ of an infinitely large (plane) plate of thickness H is a suitable model, $\gamma_p(r, H) = 1 - r/(2H)$, if $0 \le r \le H$ and $\gamma_p(r, H) = H/(2r)$, if $H \le r$. Indeed, the curvature of γ_p possesses a maximum at $r = r_s = H$. So, the assumption of compact thin layers of a height H of metal particles, randomly arranged at certain pore-wall-places, follows. In fact, $r_s \approx H$, which further can be checked by closer analysis of the maximum of $r \cdot \gamma(r)$, $r_s \cdot \gamma(r_s) \approx H/2 = 0.4$ nm. Thus, $S/V = 4/H \approx 5\ \text{nm}^{-1}$. From a formal point of view, a specific surface area $S/m \approx 200\ \text{m}^2\ \text{g}^{-1}$ results. However, only the outer side (half of this value) represents an active surface area for catalytic reactions. The ratio, $S/m = 100\ \text{m}^2\ \text{g}^{-1}$, yields a Pt dispersion $D = 100/275 \approx 0.4$.

The same is obtained by analysis of the asymptotic behaviour of the scattering intensity, where the behaviour of $I(h)$ for $0.7\ \text{nm} < h$ has been checked (so-called theory of wetted samples) [7,22–24]. The distribution law $f(H)$ obtained without any *a priori* assumptions (figure 3) [19,21], can be approximated by the density model $f(H)$,

$$f(H) \sim \frac{2\pi \cdot H^2}{\mu^3} \cdot \exp\left(-\frac{H^4}{\mu^4}\right). \qquad (4)$$

The best fit yields $\mu = 0.73$ nm. The first moment $\overline{H} = 0.8$ nm results via equation (4).

4. Discussion

The analysis of selected, deciding r-intervals ($r < L = 5$ nm and $r < L_0 = 10$ nm) has allowed to characterize the supported catalysts even for such an extremely low platinum content. The mechanism of growth and the distribution of the metal particles in the S2-system differ from that in the S1-samples.

Due to the smaller pore sizes in the S2-samples, the growth of Pt-crystallites inside the pores is very

restricted and limited. In S2(Pt), probably only a small number of Pt atoms can form crystals, which "unlimitedly" grow three-dimensional and finally form more or less idealized crystallites of ≈ 3 nm in diameter. Thus, in S2(Pt) the main part of Pt-supply should deposit at selected places as a thin Pt-skin. Clearly, in contrast to S1(Pt), here, each determination of $f(d)$ assuming spherical metal particles would include a wrong model.

We succeeded in characterizing the supported catalysts, without applying special pre-preparing procedures like pore masking (support pore packing by a liquid whose electron density is close to that of the support material, like alkyl iodides). The two systems S1/S1(Pt) and S2/S2(Pt) investigated by use of nitrogen adsorption and small-angle scattering differ essentially.

In the case of the S1-samples surprisingly clear effects result. This is based on a more or less crowded arrangement (of a typical diameter up to $L = 5$ nm) of single, nearly spherical crystallites possessing a mean chord length $\bar{l} = 1.5$ nm and a mean diameter $\bar{d} = 2.8$ nm. Assuming $L_0 = 10$ nm, here, we succeeded in calculating their size distribution density $f(d)$ (figure 2), which can be approximated by the *log normal distribution* equation (3). The reason for such a highly unsymmetrical distribution seems to be simple: The starting particle growth is nearly unlimited, but the further growth of Pt-crystallites happens under a certain restriction of free space available. Thus, the frequency of bigger diameters is overproportional suppressed.

In the case of the S2-samples the SAS curves are influenced by the metal particles as well, but by another mechanism. Here, in a first approximation, really the same pure porous glass has been investigated two times, S2 $\approx$ S2(Pt). Nevertheless, there exist additional Pt-components in the material S2(Pt). The nearly unchanged specific surface area of system S2 is defined by the morphology of the micropores of the pure glass S2. As a consequence of volume restriction, instead of globular metal particles very thin plane regions of thickness H are formed, partly covering the carrier inside and outside the pores. The random thickness parameter H can be described by a specific distribution law $f(H)$, figure 3 and equation (4). The sample S2(Pt) possesses a dispersion $D \approx 0.4$, which is more than twice the dispersion of the S1(Pt) sample, where $D \approx 0.15$ has been obtained.

5. Conclusions

The texture parameters of the porous glasses obtained by nitrogen adsorption are sufficient for selecting L [25,26]. This step allows to interpret scattering curves of the catalyst supports before and after a modification with the active component Pt.

With system S1 the pore size allows the transport of Pt-atoms to any position inside or outside the pores, followed by an undisturbed three-dimensional growth of Pt-crystallites up to a certain maximum size. In a first approximation this is not influenced by the pore openings. Global particles result, but, due to the limited space for the crystal growth, the size distribution is highly unsymmetrical.

With system S2 the existence of smaller pores influences the growth of Pt-crystallites. A three-dimensional growth is suppressed. The morphology of the support enforces the arrangement of the Pt-atoms as thin layers, simply caused by the narrower pore spaces of the support. Segments of plane "films", which are homogeneously distributed over the whole support, result. Their lateral dimensions directly depend on the typical dimension of the porous support material. Already if 2.3 nm $\lesssim r$, the structure parameters of the three-phase system (pores, SiO_2, thin Pt-film) are strongly intermixed. The intermixing is complete for 5 nm $< r$. Similar experiments should be successful for investigating Ni catalysts and others.

References

[1] Z. Konya, V.F. Puntes, I. Kiricsi, J. Zhu, P. Alivisatos and G.A. Somorjai, Catal. Lett. 81 (2002) 137.
[2] A.G. Boudjahem, S. Monteverdi, M. Mercy, D. Ghanbaja and M.M. Bettahar, Catal. Lett. 84 (2002) 115.
[3] F.B. Rasmussen, A.M. Molenbroek, B.S. Clausen and R. Feidenhans, J. Catal. 190 (2000) 205.
[4] G. Bergeret and P. Gallezot, in: *Handbook of Heterogeneous Catalysis*, Vol. 2, eds. G. Ertl, H. Knözinger and J. Weitkamp, Wiley-VCH, Weinheim, 1997, pp. 439–464.
[5] T. White, P. Kirlin, K. Gould and H. Heinemann, J. Catal. 25 (1972) 407.
[6] V.N. Kolomiichuk, React. Kinet. Catal. Lett. 20 (1982) 123.
[7] W. Gille, D. Enke and F. Janowski, J. Phys. Chem. Solids (in press).
[8] G. Porod, in: *Small-Angle X-ray Scattering*, eds. O. Glatter and O. Kratky (Academic Press, London, 1982) p. 34.
[9] L.A. Feigin and D.I. Svergun, *Structure Analysis by Small-Angle X-Ray and Neutron Scattering* (Plenum, New York, 1987) p. 107.
[10] W. Gille, D. Enke and F. Janowski, J. Porous Mater. 8 (2001) 111.
[11] D. Enke, K. Otto, F. Janowski, W. Heyer, W. Schwieger and W. Gille, J. Mater. Sci. 36 (2001) 2349.
[12] D. Jeulin, Image Anal. Stereol. 21 (Suppl. 1) (2002) S31.
[13] A. Delarue and D. Jeulin, Image Anal. Stereol. 20 (2002) 181.
[14] W. Gille, Waves Random Media 12 (2001) 85.
[15] A. Rosiwal, Verh. K.K. Geol. Reichsanst. 5 (1898) 143.
[16] C. Kittel, *Introduction to Solid State Physics* (John Wiley and Sons, Inc., New York, 1973).
[17] K.S.W. Sing and J. Rouquerol, in: *Handbook of Heterogeneous Catalysis*, Vol. 2, eds. G. Ertl, H. Knözinger, J. Weitkamp (VCH Weinheim, 1997) p. 427.
[18] F. Janowski and D. Enke, in: *Handbook of Porous Solids*, eds. F. Schüth, K.S.W. Sing and J. Weitkamp (VCH Weinheim, 2002) p. 24.
[19] I.S. Fedorova and P.W. Schmidt, J. Appl. Cryst. 11 (1978) 405.
[20] W. Gille, Particle and Particle Syst. Charact. 12 (1995) 123.

[21] W. Gille, in: *X-Ray Investigations of Polymer Structures II*, ed. A. Wlochowicz 2–5 December 1999, Sczirk, Poland, Proc. of SPIE 4240 (2000) 14 (Washington).
[22] S. Ciccariello, J. Appl. Cryst. 24 (1991) 509.
[23] S. Pikus and E. Kobylas, S. Ciccariello, J. Appl. Cryst. (in press).
[24] B. Deme and D. Marchal, J. Appl. Cryst. (in press).
[25] D. Stoyan, Image Anal. Stereol. 21 (Suppl. 1) (2002) S41.
[26] W. Gille, Mater. Chem. Phys. 77 (2002) 612.